KATHOLIEKE UNIVERSITEIT
LEUVEN

FACULTEIT WETENSCHAPPEN
Departement Natuurkunde en Sterrenkunde
Instituut voor Kern- en Stralingsfysica

Ion optics and beam transport simulations for the Collinear Resonance Ionisation beam line at ISOLDE

door

Wannes VANDERHEIJDEN

Promotor: prof. dr. G. Neyens
Co-promotor: dr. K.T. Flanagan
Begeleider: Pieter Vingerhoets

Proefschrift ingediend tot het behalen van de graad van Master in de Fysica

Academiejaar 2009-2010

Acknowledgements

Aan alles komt een einde, zo ook aan dit avontuur, dat mijn studie fysica toch wel was, met als hoogtepunt van het avontuur ongetwijfeld deze thesis. En bij het eind van zo'n avontuur horen ongetwijfeld enige bedankjes, want alleen was het nooit gelukt.

Eerst en vooral wil ik mijn promotor prof. dr. Gerda Neyens bedanken. Ze gaf me de mogelijkheid om te werken aan een nieuw project vol met uitdagingen en mogelijkheden. De trips naar CERN die ik mocht maken, waren heel leerrijk, leuk en zeker ook nuttig voor mijn thesis.

This brings me to ISOLDE, where my co-promotor Kieran is stationed. Thanks for all the help and advice for my thesis, the things you taught me about CRIS, and the good times in CERN and Geneva. I also would like to thank Andy, for the help with the technical drawings, the things he taught me, and the fun times during the construction of CRIS.

Natuurlijk zijn er nog een hele hoop mensen in Leuven die ik moet bedanken. Bedankt aan mijn begeleider Pieter, voor de hulp als ik ergens iets niet snapte, suggesties, en vooral bedankt om regelmatig achter mijn veren te zitten. En ook bedankt aan de rest van de mensen van de nuclear moments group: Marieke, voor de gezellige babbels en advies. Maarten, voor de gezellige momenten op de bureau, zeker toen we daar met twee zaten. Thanks to Mustafa for the (sometimes) profound discussions and the company in the office, and to Jasna for the pleasant chats.

Zes jaar Leuven is natuurlijk meer dan alleen studeren, ik wil mijn jaargenootjes bedanken voor de fijne jaren in Leuven, de bezoekjes aan de Domus, de Winabar en de cantussen: bedankt Katrien, Maarten, Maarten, Hans, Thomas, Peter ,Geoffrey en Steven.
Student ben je natuurlijk pas echt als je op kot zit, en als je op zo'n toffe gang zit als in Cit blok 8 gang 3 dan is het nog leuker: Bedankt Melissa, Steven, Koen, Bram, Alex, Daan, en Tom.
Natuurlijk mag ik het thuisfront niet vergeten: bedankt Nick en Tom voor de gezellige weekend avonden in De Wemeling bij een goed glas Gageleer.

Als laatste en ongetwijfeld meest belangrijke wil ik mijn ouders bedanken, omdat ze mij de mogelijkheid gegeven hebben om te gaan studeren, en omdat ze me altijd zijn blijven steunen.
Bedankt Moeke en Papa!

Samenvatting

Het werk gedaan in deze thesis past in het onderzoek van de nuclear moments group van het Instituut voor Kern- en Stralingsfysica. Daar wordt onderzoek gedaan naar de magnetische en elektrische momenten van exotische kernen. Dit zijn radioactieve kernen met een ongewone verhouding tussen het aantal protonen en neutronen. Hoe verder we weg gaan van de stabiele kernen, hoe korter de levensduur wordt, hoe moeilijker het wordt om de kernen te produceren en dus hoe lastiger het wordt om ze op te meten. Daarom zijn er nieuwere, meer efficiënte en gevoeligere technieken nodig.
De nieuwe CRIS(Collinear Resonant Ionization Spectroscopy) opstelling in ISOLDE(CERN) is zo een techniek. Om ten volle gebruik te kunnen maken van de techniek is het echter belangrijk dat de kernen ook effectief tot op het einde van de opstelling geraken waar ze gedetecteerd kunnen worden. Hiervoor zijn simulaties nodig van de ionen optica en de transmissie.

Deze simulaties worden beschreven in deze thesis. De belangrijkste bevindingen staan in hoofdstuk 5 verzameld. Er is gezocht naar de optimale instellingen voor alle elementen in de opstelling, maar dit alleen was niet genoeg: door alleen gebruik te maken van de elementen die oorspronkelijk aanwezig waren in de opstelling was het verlies van ionen onacceptabel groot, en er moest dus naar oplossingen gezocht worden.
De belangrijkste resultaten zijn de toevoeging van twee nieuwe elementen: een quadrupole doublet voor het focussen van de ionen en een extra paar afbuigplaten om de ionen terug te aligneren met de

opstelling. Met behulp van deze toevoegingen was het mogelijk om het overgrote deel van de ionen tot op het einde van de opstelling te krijgen.

Contents

List of Figures

LIST OF FIGURES

List of Tables

LIST OF TABLES

1

Introduction

The work in this thesis is part of the research programme of the Nuclear Moments group at the Instituut voor Kern- en Stralingsfysica of the Katholieke Universiteit Leuven. This research is oriented on the study of the structure of exotic nuclei by determining their ground state properties, namely the isotope shift, spin, magnetic dipole moment and electric quadrupole moment. This is done by measuring the hyperfine structure of the atomic system.

To measure more exotic nuclei that are further from stability and have lower production yields, new detection techniques with higher sensitivity are needed. One such technique is Collinear Resonant Ionisation Spectroscopy (CRIS). The new CRIS beamline is at this moment under construction at ISOLDE (CERN). Commissioning is planned in September 2010.
The goal of this thesis is to optimize the transmission of the ions in the beamline from the starting point after the beam cooler/buncher through the different experimental devices to the detection setup at the end of the beamline. At the start of my thesis, in April 2009, the construction had just started. The initial design of the beamline was used as the starting input for the simulations. Results from these simulations were used to adapt the beamline and add extra ion optics elements.

- Hyperfine interactions and nuclear moments are discussed in chapter 2
- In chapter 3 different laser spectroscopy techniques are explained, and a short overview of the CRIS beamline at ISOLDE CERN is given.
- In chapter 4 an overview is given of the SIMION software that is used for the simulations of the beam transport and ion optics. Some problems are pointed out and the limitations of the software are discussed.
- In chapter 5, the simulations of the beam transport and ion optics are explained and results are given.
- Finally the conclusions are given in chapter 6

2

Hyperfine Interactions

In this chapter a short overview of hyperfine interactions and nuclear moments is given.

2.1 Hyperfine interactions

Hyperfine interactions originate from the coupling of atomic electrons to the nucleus. This coupling gives rise to a splitting and shift of the electronic energy levels. The size of the splitting and the shift depends both on the properties of the electron cloud of the atom and on the atomic nucleus.

2.1.1 The isotope shift

The isotope shift is a small shift(typically 1:10^6 and smaller [Kin84]) in the transition frequency for a certain atomic transition i between different isotopes A and A' of the same element (see fig. 2.1). This difference originates from two effects: the change in mass of the nucleus and the change in the charge distribution of the nucleus. The first part is called the mass shift, the second the field shift [Kin84].

$$\delta\nu_i^{A,A'} = M_i \frac{m'_A - m_A}{m'_A m_A} + F_i \delta\langle r^2\rangle^{A,A'} \tag{2.1}$$

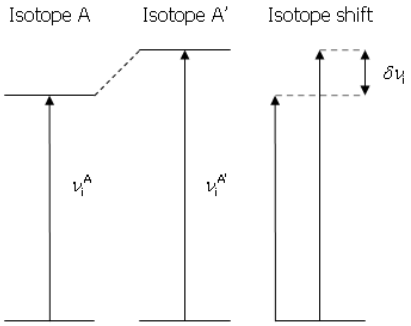

Figure 2.1: The isotope shift - Schematic representation of the isotope shift. The isotope shift $\delta\nu_i$ is given by the difference in transition frequency between the atomic levels of two isotopes A and A' of the same element.

The mass shift

The mass shift itself also consists of two parts, the normal mass shift(NMS) and the specific mass shift(SMS). The normal mass shift takes into account the effect of the reduced mass of the electron-nucleus system on the transition frequency. It is given by

$$\delta\nu_{NMS}^{A,A'} = m_e \nu_0^i \frac{m'_A - m_A}{m'_A m_A} \tag{2.2}$$

with ν_0^i the transition frequency for an infinitely massive nucleus and m_e the electron mass.

The specific mass shift comes from the correlated motion of the electrons. The specific mass shift is more difficult to calculate, but is (in first order) also proportional to the reduced mass.

$$\delta\nu_{SMS}^{A,A'} = S_i \frac{m'_A - m_A}{m'_A m_A} \tag{2.3}$$

So we can split the mass shift into a normal (N_i) and a specific (S_i) mass shift, with M_i the total mass shift constant (eq 2.4). Due to the $1/m^2$ dependence the mass shift is small for heavy nuclei.

$$\delta\nu_{MS}^{A,A'} = (N_i + S_i)\frac{m'_A - m_A}{m'_A m_A} = M_i \frac{m'_A - m_A}{m'_A m_A} \tag{2.4}$$

The mass shift not interesting from a nuclear physics point of view, because it has only a small effect on the transition frequency, and we could not obtain any interesting information on the mass of the nucleus. Furthermore there are more precise ways to measure the mass of different isotopes.

The field shift

The field shift arises from a change in the charge distribution of the nucleus in two isotopes(or isomers). It can be (in first order [Sel69]) attributed to the change in the mean square charge radius of the nucleus (eq. 2.5).

$$\delta\nu_{FS}^{A,A'} = F_i \delta\langle r^2\rangle^{A,A'} \tag{2.5}$$

Where the mean square charge radius is given by:

$$\langle r^2\rangle = \frac{\int_0^R \rho(\mathbf{r})\mathbf{r}^2 d\mathbf{r}}{\int_0^R \rho(\mathbf{r}) d\mathbf{r}}. \tag{2.6}$$

F_i is the field shift constant and is an electronic factor which has to be either calculated theoretically or semi-empirically [Neu06], and is often not well known. The effect is largest for $s_{1/2}$ electrons since they have the highest probability of overlap with the nucleus. Sudden changes in the mean square charge radius can reveal changes in the nuclear structure.

2.1.2 The nuclear magnetic dipole interaction

A second contribution to the hyperfine interaction comes from the coupling of the nuclear dipole moment with a magnetic field created by the orbiting electrons around the nucleus. Electrons with a total angular momentum J≠0 induce a magnetic field at the nucleus. The magnetic moment of the nucleus is induced by the motion of the charged protons (orbital magnetic moment) and by the intrinsic spin of both neutrons and protons (spin magnetic moment). The magnetic dipole operator is defined as [Neu06]

$$\boldsymbol{\mu} = \sum_{i=1}^{A} g_l^i \mathbf{l}^i + \sum_{i=1}^{A} g_s^i \mathbf{s}^i \tag{2.7}$$

The free-nucleon gyromagnetic ratio for a neutron and a proton are: g_l^π=1, g_l^ν=0 for the orbital part and g_s^π=+5.587, g_s^ν=-3.826 for the spin part. The magnetic dipole moment is the expectation value

$$\mu_I = \langle I, m = I|\boldsymbol{\mu_z}|I, m = I\rangle \tag{2.8}$$

For a single unpaired nucleon outside a closed shell the magnetic moment depends on the total angular momentum **j** and its orbital momentum **l**, these are called the Schmidt moments and are given by:

$$\mu(l + 1/2) = [(j - \frac{1}{2})g_l + \frac{1}{2}g_s]\mu_N \tag{2.9}$$

$$\mu(l - 1/2) = \frac{j}{j+1}[(j + \frac{3}{2})g_l - \frac{1}{2}g_s]\mu_N \tag{2.10}$$

2.1.3 The nuclear electric quadrupole interaction

This contribution comes from the interaction of the nuclear electric quadrupole moment with an electric field gradient produced by electrons with a total angular momentum J≥1. The nuclear electric quadrupole moment originates from a non spherical charge distribution of the nucleus. The z-component of the quadrupole operator in a spherical tensor basis is the zeroth order component of a rank 2 tensor, and is given by [Ney03]:

$$\mathbf{Q_2^0} = \sqrt{\frac{16\pi}{5}} \sum_{i=1}^{A} e_i r_i^2 Y_2^0(\theta_i, \phi_i) \tag{2.11}$$

The only parameter that easily is experimentally available is the spectroscopic quadrupole moment, and it is the expectation value of $\mathbf{Q_2^0}$:

$$Q_s = \langle I, m = I|\mathbf{Q_2^0}|I, m = I\rangle = \sqrt{\frac{I(2I-1)}{(2I+1)(2I+3)(I+1)}}(I||\mathbf{Q}||I) \tag{2.12}$$

The last term in this equation is called the intrinsic quadrupole moment, and is related to the deformation of the nucleus. From this equation we can see that although a nucleus can have a deformation(and thus an intrinsic quadrupole moment) the spectroscopic quadrupole moment can be zero if I<1, and thus the

deformation cannot be measured with the quadrupole moment.
Nuclei with a prolate deformation, like a rugby ball, have a positive quadrupole moment. Nuclei with a oblate deformation, like a disc, have a negative quadrupole moment.

2.1.4 The hyperfine structure

Due to the interaction of the electrons with the nuclear dipole moment and the nuclear quadrupole moment the electronic levels are split. The splitting is governed by the quantum number **F** which originates from the coupling of the nuclear spin (**I**) with the electronic spin (**J**).

$$\mathbf{F} = \mathbf{I} + \mathbf{J} \tag{2.13}$$

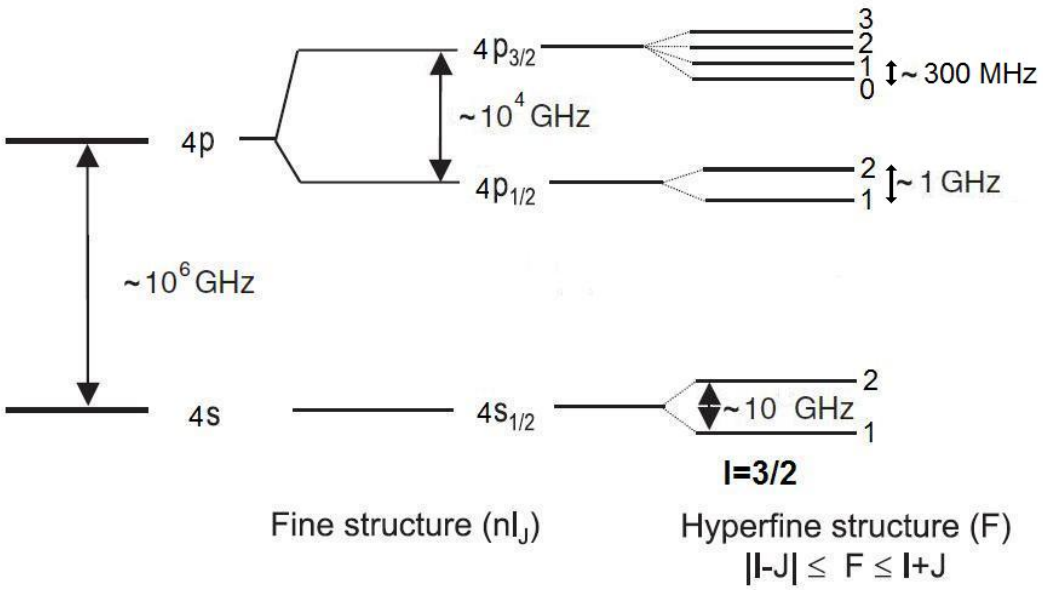

Figure 2.2: The hyperfine structure for a Cu atom with spin I=$\frac{3}{2}$ - In the middle the fine structure is shown, at the right the hyperfine structure is shown. Figure taken from [Ory09].

This allows values for F: $|I-J| \leq F \leq I+J$, so there are 2J+1 or 2I+1 hyperfine

levels if J<I or J>I respectively. The energy difference in comparison to the fine structure level for each hyperfine level is given by [Neu06]:

$$E_F = \frac{1}{2}AC + B\frac{\frac{3}{4}C(C+1) - I(I+1)J(J+1)}{2I(I-1)J(2J-1)} \tag{2.14}$$

$$C = F(F+1) - I(I+1) - J(J+1) \tag{2.15}$$

The magnetic dipole interaction constant A and the electric quadrupole interaction constant B are given by:

$$A = \frac{\mu_I B_e(0)}{IJ} \tag{2.16}$$

$$B = eQ_s V_{zz}(0). \tag{2.17}$$

Where μ_I and Q_s are the magnetic dipole moment and the spectroscopic quadrupole moment of the nucleus as defined before. $B_e(0)$ and $V_{zz}(0)$ are respectively the magnetic field and the electric field gradient at the nucleus due to the orbiting electrons.

When the nuclear spin I is not known, this can be determined either by the number of levels (when I<J) or by the relative distances between the hyperfine levels.

3

Laser Spectroscopy

In this chapter some different laser techniques for measuring nuclear moments and isotope shifts of (radioactive) nuclei are given to compare them with the CRIS technique. These techniques all use the interaction of a laser with the atomic system. By recording when the lasers are on resonance with the hyperfine structure of the atom, information about the A and B parameters and the isotope shift is obtained. From these hyperfine parameters the nuclear moments are deduced. First Resonant Ionisation Spectroscopy (RIS) is explained, then Collinear Laser Spectroscopy (CS). And finally Collinear Resonant Ionisation Spectroscopy (CRIS). An overview of the new CRIS beamline at ISOLDE is also given.

3.1 Resonant Ionisation Spectroscopy

The Resonant Ionisation Spectroscopy(RIS) technique stepwise ionizes the atom using pulsed lasers [Alk92]. To achieve an element selective ionisation a multi step process is needed. The atomic energy levels are different for each element and with the appropriate choice of the laser frequencies only a specific element is resonantly excited and subsequently ionized. The resonantly ionized ions can then be accelerated and mass separated by a dipole magnet. This allows a specific isotope to be selected by the appropriated choice of element(Z) and mass(M). This technique can be used as an ion source for other experiments (see figure 3.1). If a tunable narrow bandwidth($\tilde{1}$GHz) laser is used in the resonant excitation step and if its transition frequency is scanned, one can scan the hyperfine structure of

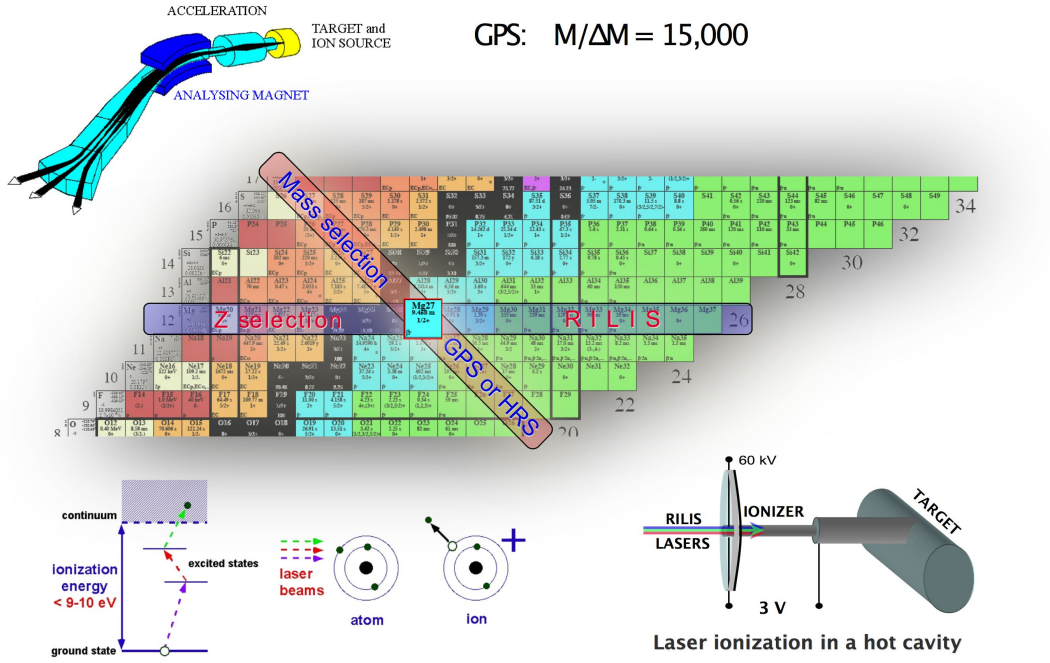

Figure 3.1: RILIS - By using resonant excitation steps, an electron is excited and subsequently ionized, this way an element selective way of ionisation is achieved. By using a tuneable laser, the hyperfine structure can be scanned. Figure taken from [RIL]

the electronic levels. The resolution of this technique is limited by the Doppler broadening due to the spread in energy of the atoms from the ion source thermal motion (which corresponds to typically 4-5GHz in spread). This way transitions that are close to each other can not be resolved, and it is not possible to measure the quadrupole splitting in the hyperfine spectrum. This way it is difficult to measure the spin unambiguously.

The big advantage of this technique is that the detection sensitivity is high because of the high detection efficiency for ions. Once the atoms are ionized and mass separated they can be transported to a detection setup where either the ions themselves or the radioactive decay of the ions is measured, atoms with yields as low as 1 ion/s can be investigated [Alk92].

3.2 Collinear Laser Spectroscopy

Another laser technique widely used is Collinear Laser Spectroscopy (CS), the method was developed more then 30 years ago [Kau76; Win76], and is still used today. The setup consists of a accelerated (30-60kV) ion or atom beam that is overlapped with a laser beam collinearly. The scanning of the transition frequency is done by Doppler tuning the ion beam (see eq. 3.1). While the frequency of the laser(ν_L) is kept stable the ions are accelerated or decelerated by a potential (U) so that the frequency seen in the rest frame of the ions or atoms(ν) is scanned due to the difference in Doppler shift for the different velocities.

$$\nu = \nu_L \frac{1-\beta}{\sqrt{1-\beta^2}}, \qquad \beta \approx \sqrt{\frac{2eU}{mc^2}} \tag{3.1}$$

When the ions or atoms are on resonance, the electron cloud is excited and it de-excites through photons emission. These photons are then detected with a photo multiplier tube (PMT), which gives the measured hyperfine spectrum.

The big advantage of the collinear setup is that the acceleration suppresses the Doppler broadening from the ion source. When ions are accelerated through a constant potential the initial spread in energy remains constant. From equation

3.2 we can see that if the spread in energy (δE) is constant and the speed (v) increases, the spread in speed has to decrease (see also figure 3.2).

$$\delta E = \delta(\frac{1}{2}mv^2) = mv\delta v = constant \tag{3.2}$$

The sensitivity of this technique is lower than that of RIS, due to background

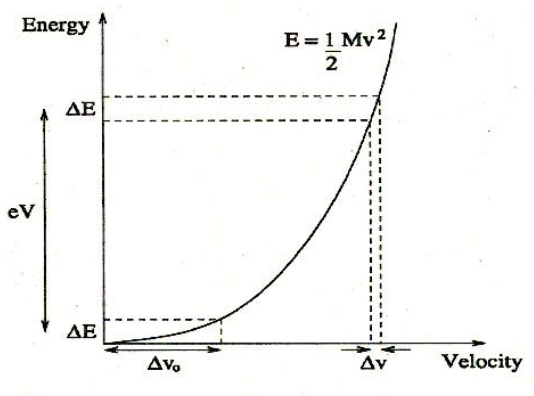

Figure 3.2: Doppler tuning - When the ion beam is accelerated through a constant potential the spread in energy remains constant and the spread in speed has to decrease.Figure taken from [Ory09].

of scattered laser light and a low detection efficiency of the isotropically emitted photons. The detection sensitivity can be increased with orders of magnitudes by bunching the beam and gating the signal when the bunch passes the detection setup. This way the background is reduced (typically 3 orders of magnitude). When using a bunched beam, typically 10^3 ions/s are needed to get data [Cam02], while when using the continuous beam 10^6ions/s are needed. While the use of the buncher greatly improves the range of isotopes that can be measured, the limit for detection is still quite high compared to RIS.

3.3 Collinear Resonant Ionisation Spectroscopy

Collinear Resonant Ionisation Spectroscopy (CRIS) is a technique that combines the high sensitivity of Resonant Ionisation Spectroscopy with the high precision of Collinear Laser Spectroscopy. It was first proposed in 1982 [Kud82], and it

uses the high detection efficiency of RIS while also using the high precision of CS. The experimental setup is very similar to the one used in CS. A fast ion beam is overlapped with a laser beam, and then neutralized. Instead of measuring the resonant fluorescence of the excited atoms, the atoms are ionized in a multistep process and the resulting ions are deflected towards a detection setup where either the ions or the radioactive decay of the ions are measured. This technique has already been tested in the past [Sch91], but the gain in detection efficiency was lost due to duty cycle losses of the continuous beam in combination with a pulsed laser. The total efficiency was therefore not much different from the classical collinear laser spectroscopy.

3.4 Overview of the new CRIS beamline at ISOLDE

The new CRIS beamline at ISOLDE CERN is currently being built. With the RFQCB (Radio Frequency Quadrupole Cooler and Buncher) ISCOOL bunched beams are available at ISOLDE, and this gives some opportunities to use the CRIS technique with higher efficiency than before. While ISCOOL cools the beam and lowers the emittance of the beam, it is the bunching of the beam that gives the biggest improvement in detection efficiency and sensitivity

Figure 3.3 shows a technical drawing of the CRIS beamline viewed from above. The bunched ions from ISCOOL come in from the right and are focussed in the quadrupole triplet. The ion beam is then bend over an angle of 34° so that it overlaps with the trajectory of the laser beam. The ions are then neutralized in the charge exchange cell, where a scanning voltage is applied to the ion beam before neutralization. Therefore the charge exchange cell is put inside a Faraday cage. Ions that are not neutralized are deflected after the charge exchange cell, otherwise they would give a background in the ion detection, since there is no way to discriminate between resonantly ionized ions and non neutralized ions. The atoms enter the interaction region where they are reionized by a multistep laser process. These ions are then deflected towards the detection setup where they will be measured. By deflecting the ions they get separated from neutral

contaminations. These isobaric contaminations are not ionized because of their different hyperfine structure.

The new beamline is designed to have Ultra High Vacuum (UHV),$<10^{-9}$mbar, in the interaction region where the laser beam interacts with the atoms and ionizes the atoms. The ultra high vacuum prevents that atoms are non-resonantly ionized by collisions with the restresidual gas left in the vacuum chambers. This would give a constant background and lower the sensitivity of the measurements. To reach the ultra high vacuum a differential pumping system is used. While there is a relatively poor vacuum in the charge exchange cell ($>10^{-5}$mbar) further down the beamline better vacuum is achieved by putting pumping apertures in the beamline and additional vacuum pumps.

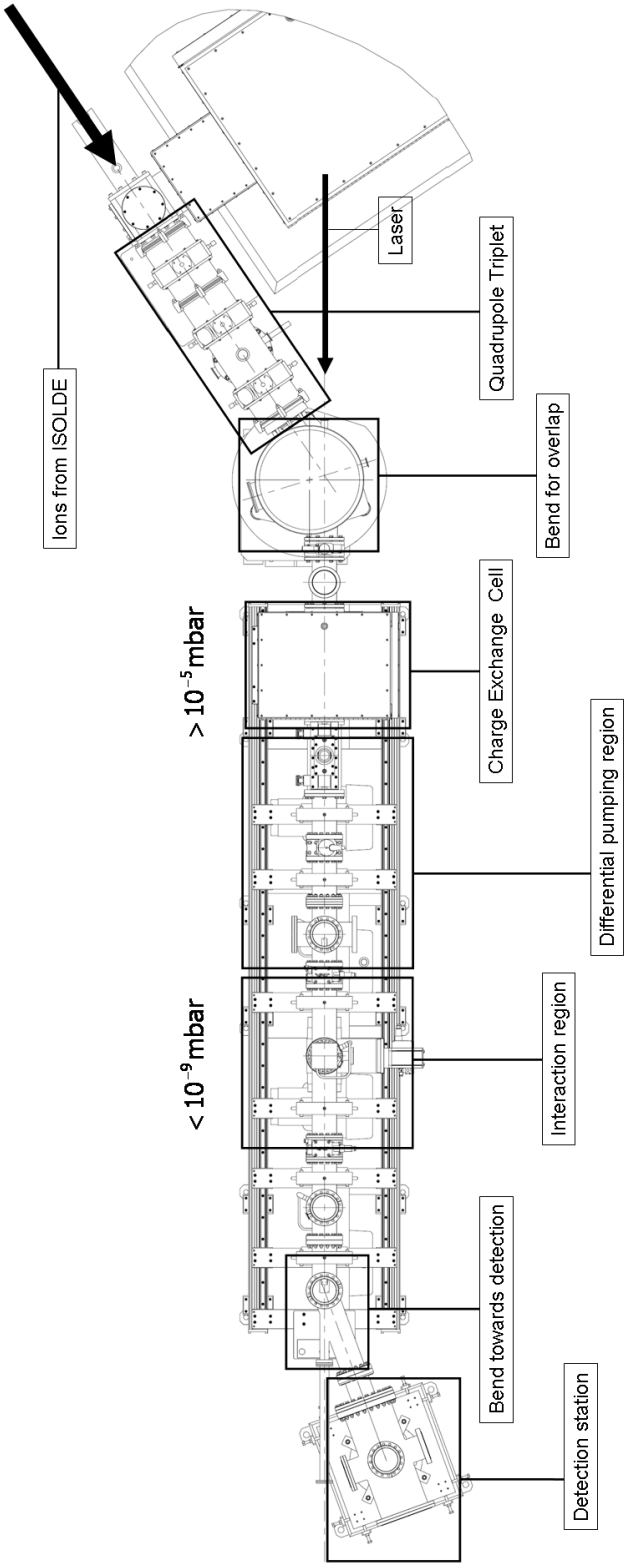

Figure 3.3: The beamline as in ISOLDE, the key parts of the set-up are indicated

4

Simulation software: SIMION

For the simulation of the beam transport and ion optics in the CRIS beamline, SIMION 8.0 was used. SIMION is a program used to calculate trajectories of (charged) particles in electromagnetic fields [SIM]. Those fields are calculated given a particular configuration of electrodes with the appropriate voltages on them. The particle trajectories and equipotential lines (see figure 4.1) can be visualized and data parameters of the particles can be recorded.

4.1 Ion Optics Workbench

The Ion Optics Workbench (.IOB) is the main file in which the whole simulation runs. It is composed of one or more sets of electrodes (called potential arrays), which are correctly positioned according to each other. The IOB also contains the starting properties of the ions (ion definitions), data recording settings and user programs. When working in the IOB file the voltages applied on the electrodes can be changed and parameters of the ions and the data recording can be adapted.

A potential array (PA) is a three dimensional grid in which each point is defined either as a non-electrode point or as an electrode point and it has a potential assigned. The electric field in non-electrode points are calculated by solving the Laplace equation with finite difference methods, this is called refining the potential array. The time it takes to refine the potential array depends on a number of parameters, but the most important are the size of the PA, the number of

adjustable electrodes and the desired precision of the calculations.

Each PA has a definite number of points in the x,y and z direction and has possibly a planar or cylindrical symmetry. By using symmetry, less points have to be used in a potential array and so the file size can be lowered. If a set of electrodes has for example a fourfold symmetry one can define the whole set by only one fourth and mirror over the appropriate planes (see figure 4.1). The use of symmetry results in smaller files and faster refinements, adjusting potentials and thus faster simulations.

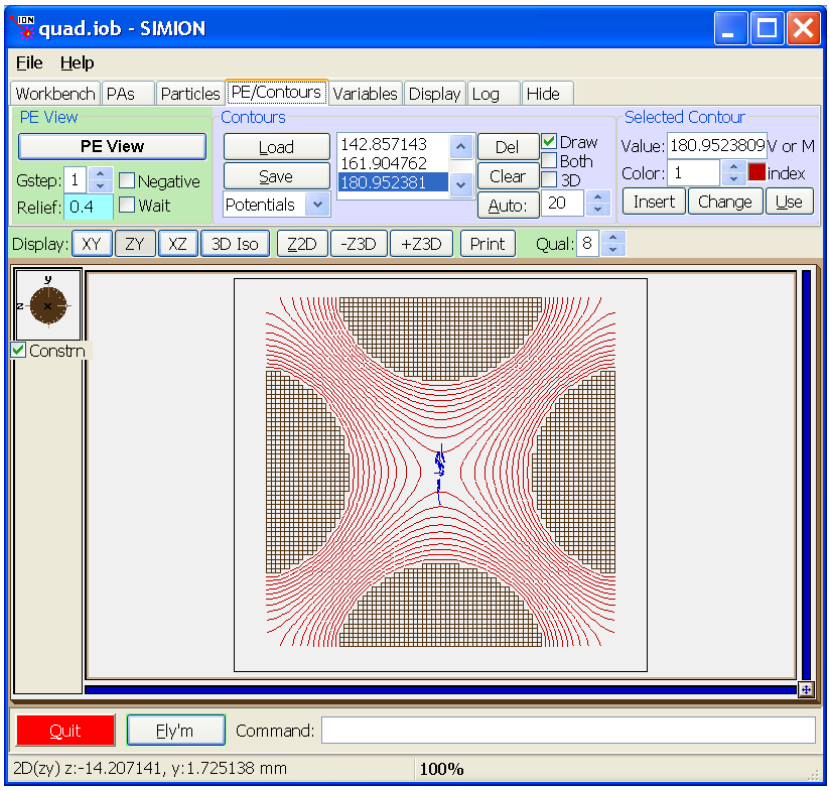

Figure 4.1: Cross section of a quadrupole with equipotential lines drawn.
- This quadrupole was made by defining only the upper right quadrant and mirroring it over the horizontal and vertical plane

4.2 Limitations of the simulations

The way SIMION works gives rise to some problems. The electric fields are only calculated inside the volume of a potential array. Therefor, to make the most correct simulations it would be best to simulate the whole setup in one potential array. However SIMION limits the maximum number of points in each PA to nearly 200 million (which corresponds to about 1.86GB memory use (SIMION uses 10 bytes for each grid point). The total memory use allowed by SIMION for a complete workbench is about 2GB. These memory restrictions make it impossible to simulate the whole setup in one PA file.

The solution for this problem consists in breaking up the beamline in smaller parts and combine them in a workbench. This way you can also use the highest possible symmetry for each part (e.g. fourfold symmetry in a quadrupole) while using no symmetry in other parts. Breaking up the beamline also allows to use different grid densities in different parts of the setup. Some regions of the setup are more sensitive to the resolution of the electrodes than other (eg the holes in the charge exchange cell which are only 6mm in diameter) and thus benefit from using a higher grid density at that place. Less important regions can use a lower grid density and so use less memory. In larger regions with no or lower symmetry lower grid density has to be used to keep the file size limited.

Since the potentials are only calculated inside the volume of the PA, the potentials at the boundary of the PA should match to the potential of the PA next to it. In practice this is most easily achieved by making sure the potential is as close as possible to 0V at the boundaries. Since all electrodes are inside the vacuum chambers which are at ground potential this is not so difficult. We only have to make sure that we take enough vacuum chamber around the electrodes into account so that the electric potentials drops to zero at the edges. This is however not possible when two sets of electrodes are too close to each other. Then we have to take multiple electrodes inside one PA, which results in bigger files and/or lower resolution. Since we cut the potentials off at the end of the PA and the potential at that point is mostly nonzero we introduce errors into the

simulation. These errors limit the precision of the simulation (most noticeable the energy of the ions), but do not significantly change the trajectories of the ions, which is the most important parameter in the simulations.

5

Simulations of the ion transport

5.1 Goal of the simulations

The goal of the simulations is to optimize the transmission of the ions through the CRIS beamline. Since we want to be able to measure ions with low production yields it is most important that the losses in the beamline are reduced to an absolute minimum. The biggest problems are the pumping apertures (which are needed for the differential pumping and are only 10mm wide) and the apertures in the charge exchange cell (which are only 6mm wide). Every ion that is too far off centre will be stopped there and will be lost, thus reducing the sensitivity of the experiment. So the beam has to be kept as small as possible at each moment and aligned with the beamline so that it reaches the detection setup.

The simulations should be treated as rough indications to show what the general effects of the electrodes in the beamline are on the position and the shape of the ion beam. There are some approximations used in the simulations (e.g. the shape of the electrodes are not exact, and the properties of the incoming ion beam from ISOLDE is approximated). This limits the accuracy of the results, but should nonetheless give a good approximation and point out possible problems. The simulations should also be a good starting point for the settings of the beam tuning for the on-line experiments. The simulations pointed out some major problems in the beamline with the alignment and the divergence of the ion beam. To solve these problems additional ion optic elements were added in the simulations. The

simulations showed that these additions are able to solve the problems that were encountered. With the information from the simulations the additional elements have been designed, built and installed in the beamline.

5.2 Electrostatic deflection of charged particles

If we look at the motion of a charged particle in an electric field perpendicular to the velocity of the particle, the force on the particle is given by:

$$m(\frac{dv}{dt}) = zeE = \frac{mv^2}{\rho} \tag{5.1}$$

Where ρ is the radius of curvature of the particle trajectory. The electrostatic rigidity χ_E or Eρ of a particle is defined by [Wol87]:

$$\chi_E = E\rho = \frac{mv^2}{ze}. \tag{5.2}$$

For non relativistic particles(v$\ll$c) which have a kinetic energy

$$E = \frac{mv^2}{2} = -zeV. \tag{5.3}$$

due to an acceleration over a potential -V, this reduces equation 5.2 to:

$$\chi_E = -V. \tag{5.4}$$

This means that particles which are accelerated over the same potential, and thus have the same energy, follow the same trajectory in an electric field, independent of their mass. This is useful when particles of different masses are used in the same experimental setup (not necessarily at the same time), as is in the CRIS setup. If the settings of the electric fields are optimized for a certain mass this setting can be reused for all other masses as long as the energy of the ion beam is not changed.

5.3 Focussing of ion beams

For focussing a charged particle beam we would like to have an electrostatic lens which has a linear increase in electric field strength when moving away from an

optical axis. This way the force on a charged particle is proportional to the distance to the optical axis and particles further away from the optical axis are deflected more than particles close to the optical axis. This way particles that enter the lens parallel to the optical axis are focussed in a single point [Wol87], much like a classic optical thin lens. An example of such a lens is a electric quadrupole. An ideal electric quadrupole lens consists of 4 hyperbolic electrodes with the opposite electrodes at the same potential and the adjacent electrodes have opposite voltages. The electric potential of this configuration is given by:

$$\mathbf{V}(x,y) = \frac{(x^2 - y^2)V_0}{r_0^2} \tag{5.5}$$

Where $\pm V_0$ is the voltage applied on the electrodes and r_0 half the distance between the electrodes. We then can calculate the electric fields in the x and y direction:

$$E_x(x,y) = -\frac{\partial \mathbf{V}}{\partial x} = -\frac{2V_0}{r_0^2}x \tag{5.6}$$

$$E_y(x,y) = -\frac{\partial \mathbf{V}}{\partial y} = \frac{2V_0}{r_0^2}y \tag{5.7}$$

This is indeed a linear increasing electric field as desired.

While a quadrupole focusses charged particles in one plane, it defocusses in the plane perpendicular to the focussing plane. To achieve an overall focus in both planes we need at least two quadrupoles, the first focussing in the horizontal plane and defocussing in the vertical plane and the other focussing in the vertical plane and defocussing in the horizontal plane. In general a quadrupole triplet is preferred over a quadrupole doublet because usually the beam profile stays rounder in the quadrupole triplet [Wol87].

The hyperbolic electrodes are often approximated by circular electrodes (see figure 5.1) or by a stepped configuration. Circular electrodes approximate the field properties of hyperbolic ones, provided that the ratio between the radius of the electrode and the distance between the tip of the electrode and the optical axis is given by:

$$\frac{R}{r_0} = 1.15 \tag{5.8}$$

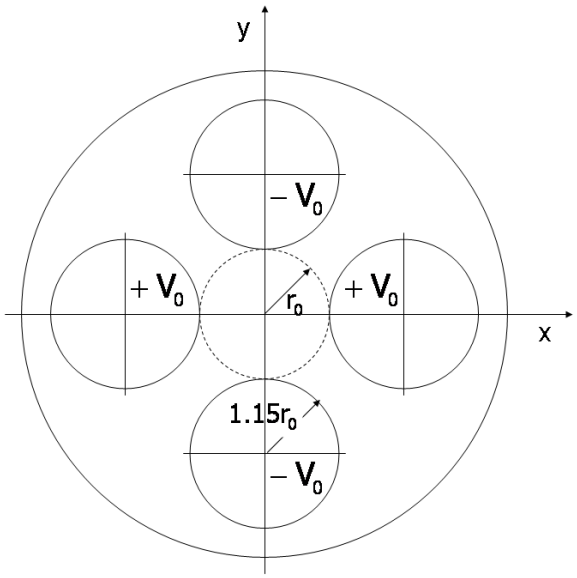

Figure 5.1: Quadrupole with circular electrodes - An electric quadrupole lens is approximated by using 4 circular electrodes instead of hyperbolic electrodes. When using the correct proportions this approximates the quadrupole field given by hyperbolic electrodes

5.4 The ISOLDE ion beam

To describe the properties of a particle beam, the emittance of the beam is used. The emittance of the beam is the volume of the beam in the particle position and momentum phase space (x,p_x,y,p_y,z,p_z). Due to Liouville's theorem the volume in phase space is conserved for conservative forces. While it may change shape, the total volume is conserved. If the motion of the particles in the beam in each direction is independent of each other, the emittance is conserved in each direction separately (see eq. 5.9).

$$\int\int dx_i dp_{xi} = constant, \qquad \int\int dy_i dp_{yi} = constant \tag{5.9}$$

The emittance in the direction parallel to the motion of the beam is called the longitudinal emittance, the emittance in the direction perpendicular to the motion of the beam are called the transverse emittances. The shape of the emittance tells us how the beam behaves. When looking at the emittance one can see if the beam is converging, diverging, parallel or in focus by looking at the shape (see figure 5.2). The emittance shape constantly changes either due to ion optic elements (bending plates, quadrupoles, etc.) or just by moving in a region without an electromagnetic field. The emittance is often represent in a plot as the distance of the particles to the optical axis in mm plotted versus the angle of the particles in mrad(see figure 5.2), this gives a total emittance expressed in mm mrad. The x axis is chosen in the horizontal plane, while the y axis is in the vertical plane.
A beam with a low emittance is desired, this means that both the size and di-

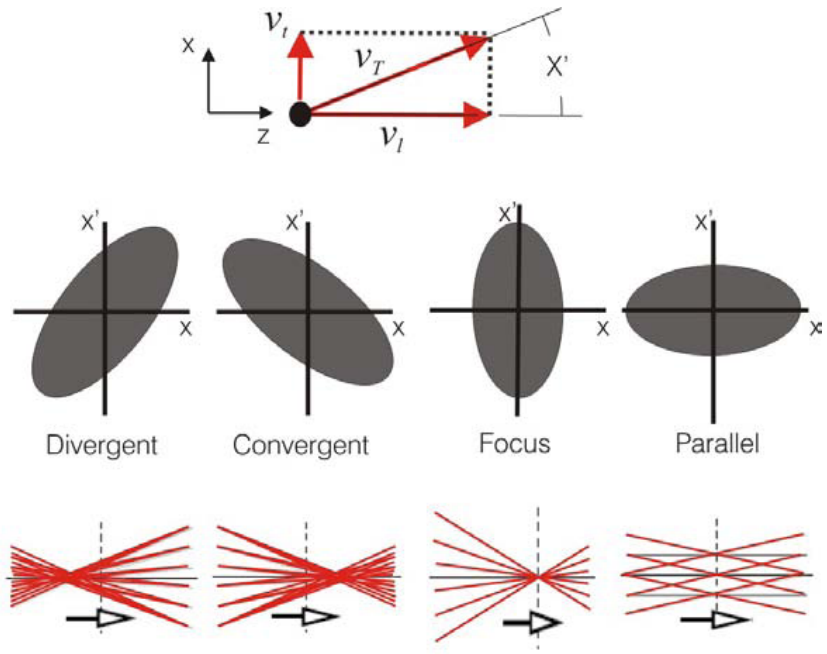

Figure 5.2: Emittance - The different shapes of the emittance correspond to different situations. Figure taken from [Pod06]

vergence of the beam are small. A beam with a big emittance quickly becomes big, and particles are lost when they hit the wall of the vacuum chamber. Since

the emittance is conserved it is important to start with an emittance as low as possible. For this reason the ion beam from ISOLDE can be cooled in ISCOOL before being send to an experiment. From emittance measurements the transverse emittance of ISCOOL was measured to be less then 3.5 π mm mrad [Man09] compared to a typical emittance of 35 π mm mrad without cooler [Jok03]. For the simulations a circular beam with a radius of 1mm and a maximum divergence of 3.5mrad was used. The energy of the beam was chosen to be 30keV, which is the normal accelerating voltage applied to ISCOOL and a mass 40 was chosen for the ions.

After the charge exchange cell there is a large drift region in which there is no more possibility for focussing the beam. To prevent losses of the beam in this region, the beam has to be as parallel as possible, so the divergence must be low. This in turn means that the size of the beam must become bigger to conserve the emittance.

5.5 Quadrupole Triplet

The quadrupole triplet at the entrance of the beamline (see figure 3.3) was already present from the previous experiment, and it was originally the only element that was foreseen in the CRIS beamline for focussing the beam. The quadrupole triplet is used in a symmetric way, which means that the same voltages are applied on the first and on the last quadrupole. The quadrupoles are convergent - divergent - convergent in the horizontal plane. The quadrupole triplet is used to minimize the diameter of the beam and produce a beam that is as parallel as possible before it goes into the 34° bending chamber or injection into the CRIS beamline. It's important that the beam is parallel, since after neutralisation the ions can't be focused anymore and the beam would become bigger and large parts would be lost. The optimal values for the quadrupole triplet derived from the simulations are:

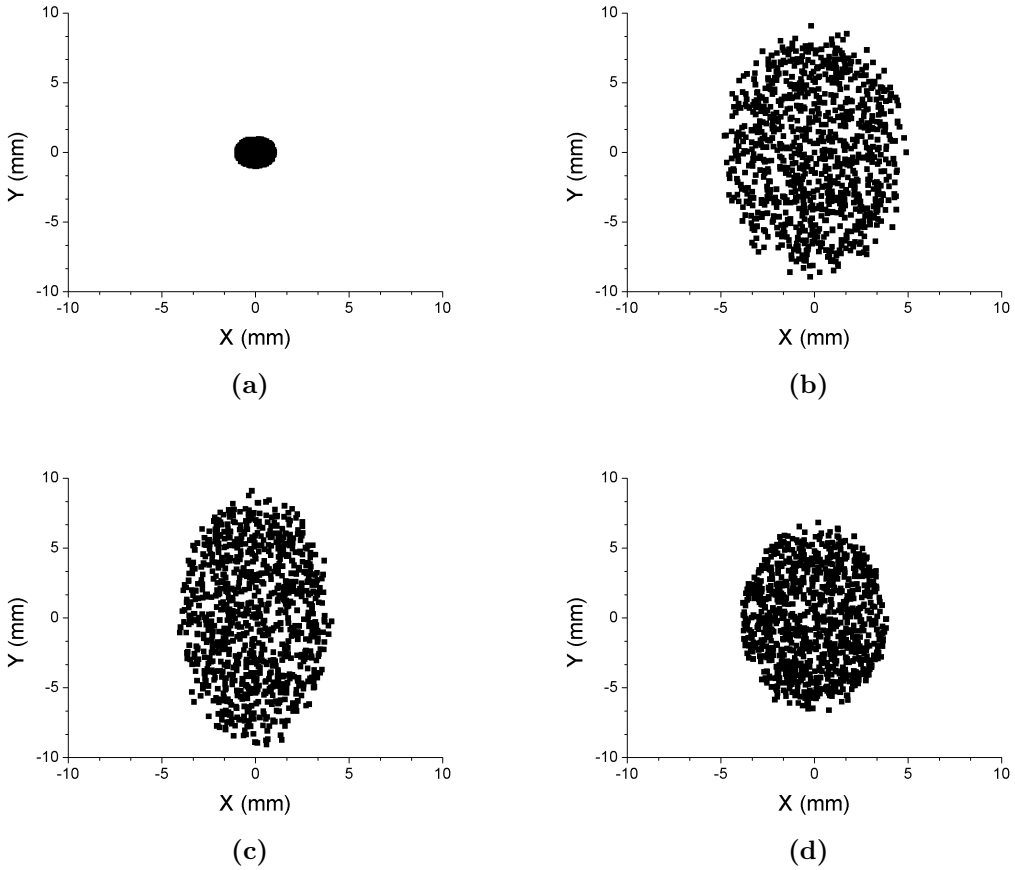

Figure 5.3: Size of the beam spot at the start of the simulation (a), in between the first and second quadrupole (b), between the second and the third quadrupole (c) and after the whole quadrupole triplet (d).

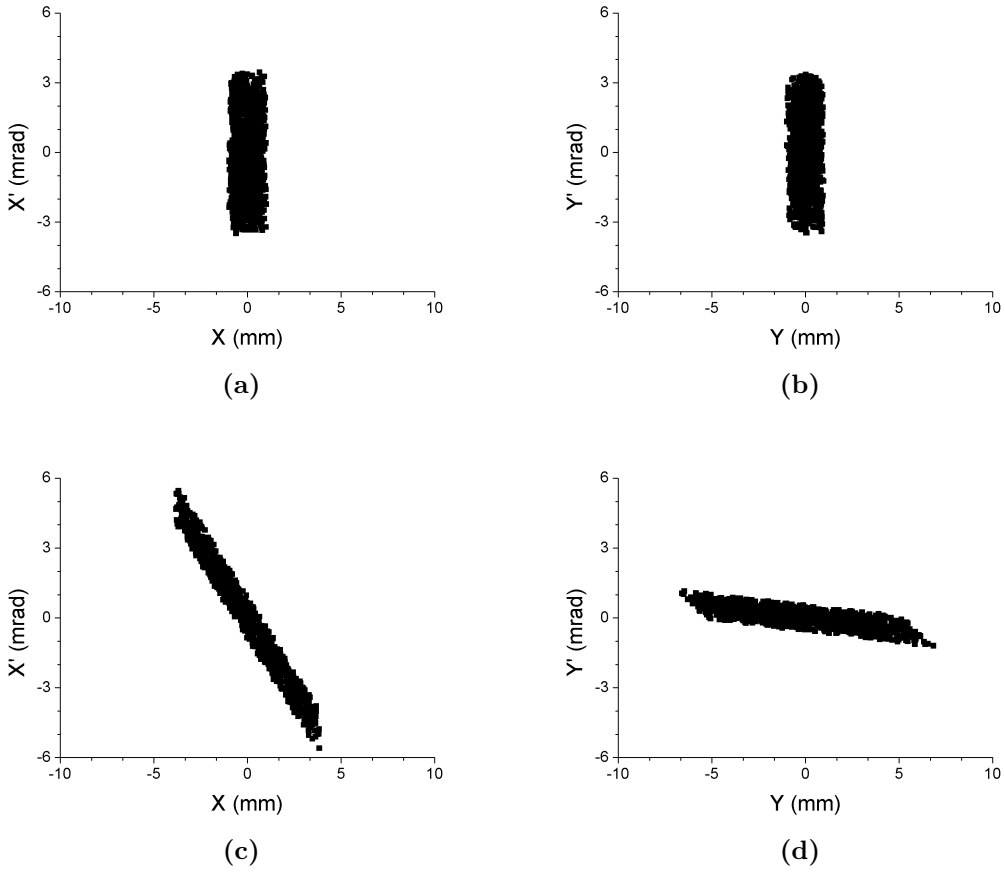

Figure 5.4: At the start the beam is in focus and small in both the horizontal direction(a) and the vertical direction (b). After the quadrupole triplet the beam is covergent in the horizontal direction (c), while in the vertical direction the beam is almost parallel (d)

Q0	Q1	Q2
±1000V	∓1250V	±1000V

Table 5.1: Optimal voltages on the quadrupole triplet

5.6 Bend for overlap with the laser

The 34° bending chamber is the next important part in the simulation of the beamline (see figure 3.3). It was also present already at ISOLDE, a left-over from the previous experiment on this beamline. It is used to bend the beam so that it overlaps with the laser beam. The bending unit consists of two parallel plates which bend over an angle of 34° and are 70mm apart (see figure 5.6). In the middle between the two plates there are two small plates at the top and the bottom for steering the beam in the vertical plane. In the bending plate on the outside there is a hole to let the laser beam enter the beamline and overlap with the ion beam. This hole disrupts the electric field between the two bending plates, but the effect on the electric field is rather small and the effect on the ion beam is negligible compared to other effects. A more important effect comes from the position of the bending unit inside the vacuum chamber. Since the bending plates are at high voltage and the vacuum chamber is at ground potential this gives rise to fringing fields outside the bending unit. Due to the asymmetrical positioning inside the vacuum chamber, the fringing fields are also asymmetric, and this gives rise to a shift of the ion beam away from the centre of the beamline. It is thus impossible to simultaneously bend the beam over an angle of 34° and keep it centred after the bending. If the beam is bent over an angle of 34° the ion beam is 8mm off centre (see figure 5.6), while if the beam is centred at the end of the vacuum chamber it is bent over an angle of 35.25° (see figure 5.7). Both deviations are a problem for the transmission of the beam. In the case of the 34° bend most of the beam is stopped when the beam hits the charge exchange cell, since the hole for the beam to pass through is only 6mm wide and is positioned in the middle of the beamline. If the bending angle is too big, the ion beam is not aligned with the beamline any more, for a 1.25° deviation this gives rise to a 65mm shift 3m further down the beamline (just before the next parallel plates),

and thus the ion beam is completely lost in the apertures. To correct for this shift extra parallel plates have been added right after the 34° bending plates (see next section).

Another problem with the bending unit is that it strongly focusses the ion beam in the horizontal plane which results in a divergence behind the focal point. To correct for this divergence, an additional focussing element (quadrupole doublet) has been added between the bending unit and the charge exchange cell(see section 5.8).

The beam is also deflected downwards by the bending unit. Without correction, the beam shifts about 2.5mm downwards when it reaches the bend toward the detection. The effect is rather small and the associated losses rather low(about 1 percent). To correct this, small voltages are applied to the electrodes in the middle of the bending unit(see figure 5.5).

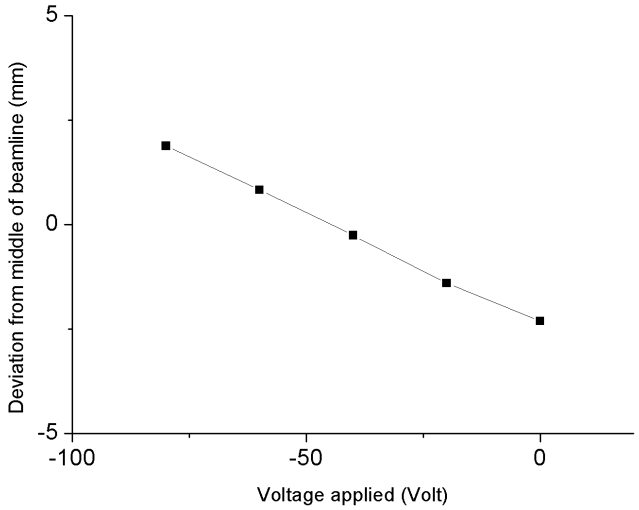

Figure 5.5: Vertical correction - Voltages applied versus the deviation from the middle of the beamline in the vertical plane

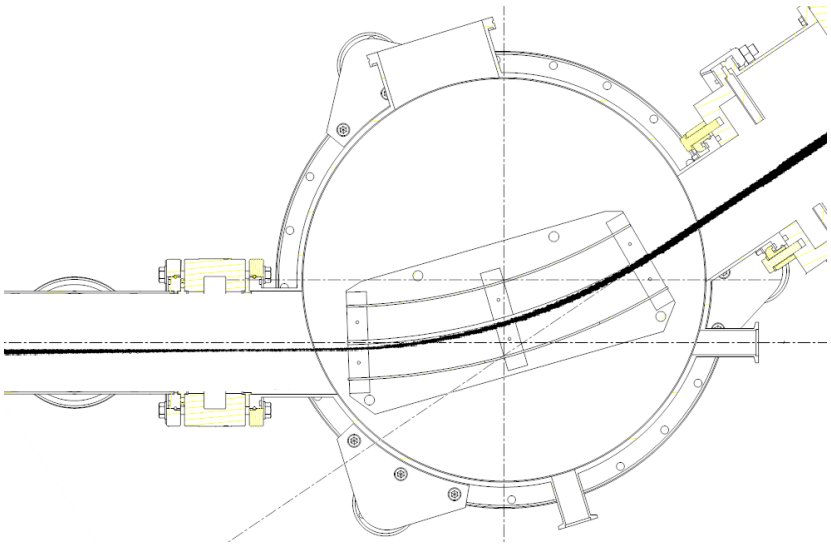

Figure 5.6: Ions bend over 34 degree - The ion beam from ISOLDE comes in from the right. When the beam is bent over an angle of 34 degree it is off centre, the centre of the beamline is marked by the dotted line.

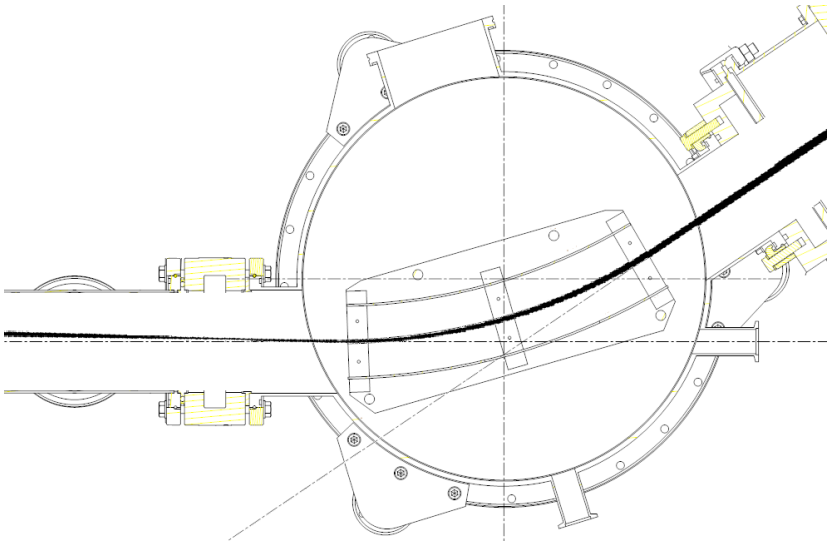

Figure 5.7: Ions bend over a larger angle - The ions are centred when they leave the vacuum chamber, but they are not aligned anymore and move away from the centre of the beamline.

5.7 Additional parallel plates

Since it was impossible to get both the angle and the position of the beam correct at the same time, extra bending plates had to be added for the correction of the beam, this provides additional degrees of freedom to manoeuvre the beam. By bending the beam over an angle that is too big, the beam can be aimed at the middle of the beamline and then be bend by the extra bending plates to correct for the wrong angle. This way, both the position and the angle of the beam can be correct and the ion beam is back aligned with the beamline. The bending plates have to be small enough to fit at the end of the vacuum chamber, without getting too close to the other bending plates.

The correct alignment was achieved by bending the beam over an angle bigger then 34° so that it is centred again, and then use the bending plates to correct the angle back to 34° so that the beam is again aligned with the beamline (see figure 5.8).The information from the simulations was used to design the extra bending plates.

Voltage		Angle	Shift
±3400V		34°	8 mm
±3610V		35.25°	0 mm
±3610V	∓550V	34°	0 mm

Table 5.2: Voltages on the bending plates and the extra bending plates, the angle of the beam and the shift from the centre of the beamline

5.8 Quadrupole doublet

To correct the beam for the divergence induced by the bending plates, an additional focussing element is needed. Because there is only a limited space available between the bend and the charge exchange cell, it is impossible to fit in a quadrupole triplet. Therefor a quadrupole doublet was chosen, although the focussing properties of a quadrupole triplet are in general better than those of a

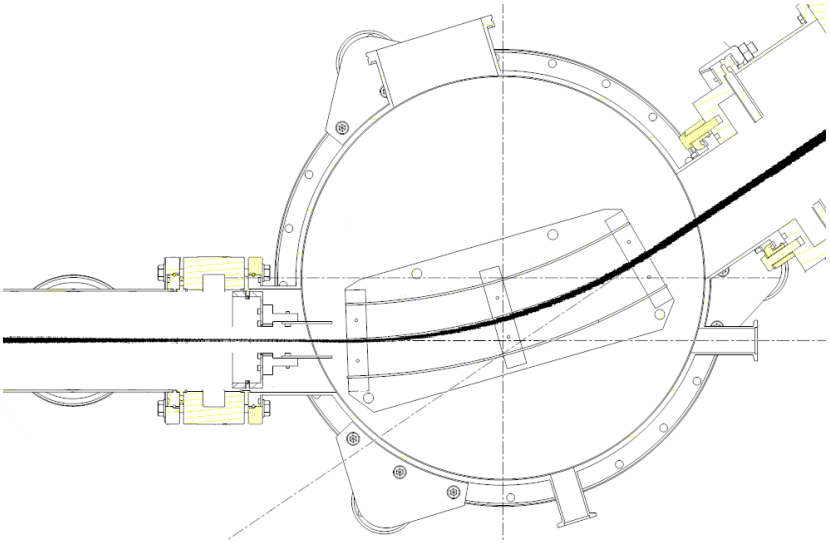

Figure 5.8: Situation with extra bending plates - Ions are centered and aligned

quadrupole doublet (the beam stays usually rounder for a triplet [Wol87]). For a comparison, the size and distance between the opposite electrodes for both the quadrupole triplet and the quadrupole doublet are given in table 5.3. With the results from the simulations a quadrupole doublet was designed (see figure 5.9) and has been built and installed into the beamline.

The quadrupole doublet consists of two identical quadrupoles. The electrodes are half cylinders with a 24mm radius, there is 42mm between the opposite electrodes and they are 40mm long. They are kept in place by a PEEK (Polyether ether ketone) support structure. This structure also keeps the two quadrupoles at a fixed distance (117mm) and maintains the correct orientation. The whole device is inserted and fits in a 4 way cross vacuum chamber between the bending chamber and the charge exchange cell.

The optimal settings for the quadrupole doublet are given in table 5.4. These values are obtained with the optimal settings for both the quadrupole triplet and the 34° bend as given in the previous sections. With these setting almost a 100% transmission of the beam was obtained.

Figure 5.9: Quadrupole doublet - the Quadrupole doublet designed according to the specification from the simulations. The electrodes are the small metal half cylinders at the top and bottom, the rest is the PEEK support structure

	Triplet	Doublet
Length	175-225 mm	40 mm
Distance	110 mm	42 mm

Table 5.3: Comparison of the length of the electrodes and distance between opposite electrodes between the quadrupole triplet and the quadrupole doublet.

5.9 Charge exchange cell

In the charge exchange cell (CEC) the ions are neutralized. In the simulations this is done by a user program, this is a small piece of code in which we can define changes in the properties of the ions that are flown in the simulations. In this case the charge of the ions is changed from +1 to 0 inside the charge exchange cell. Later in the simulation the neutral atoms are re-ionized in the interaction region.

It is important to do this, in order to get the correct energy of the ion beam after the charge exchange cell. Indeed, if a positive voltage is applied on the CEC, the

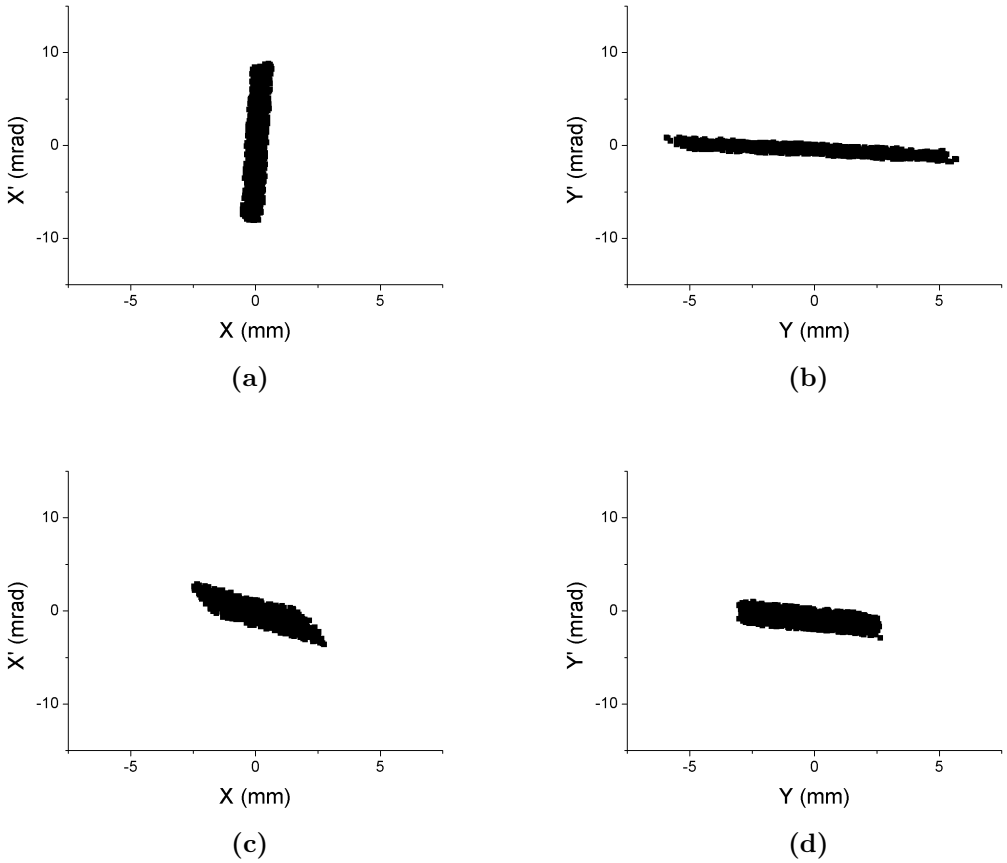

Figure 5.10: Emittance before and after the quadrupole doublet. Before the quadrupole doublet is the beam in the horizontal (x direction) plane strongly focused due to the bending plates (a). The vertical plane (y direction) is still parallel (b). After the quadrupole doublet both x and y are parallel (c) and (d).

Q0	Q1
+700V	-1200V
-700V	+1200V

Table 5.4: Optimal voltages on the quadrupole doublet

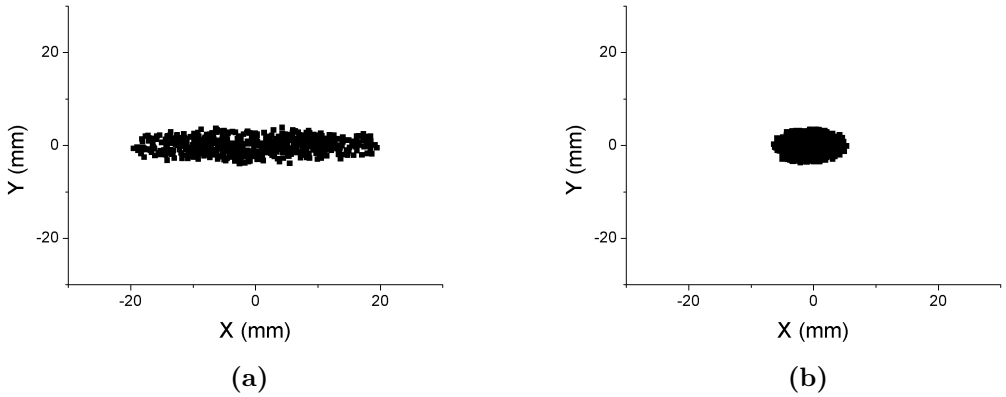

Figure 5.11: Size of the beam just before the bend towards the detection. Without the correction from the doublet the beam becomes big in the horizontal plane , and a big part of the ion beam is lost (a). With the quadrupole doublet the beam is small and losses are minimized (b)

ions are slowed down when moving towards the charge exchange cell. In the cell the ions are then neutralized so that when they leave the charge exchange cell their energy doesn't change anymore. If the ions would not be neutralized in the simulation they would accelerate again when they leave the charge exchange cell. Thus the energy and velocity of the ion beam would not be correct, which in turn affects the voltages that need to be applied to bend the reionized beam further down the beamline.

This change in energy does affect the emittance, not by increasing it, but by changing the shape. This can be seen in Figure 5.12. In the case of a large positive voltage this results in a beam that blows up faster then without the voltage applied, and this gives some loss in the total transmission to the detection setup

(see figure 5.13).

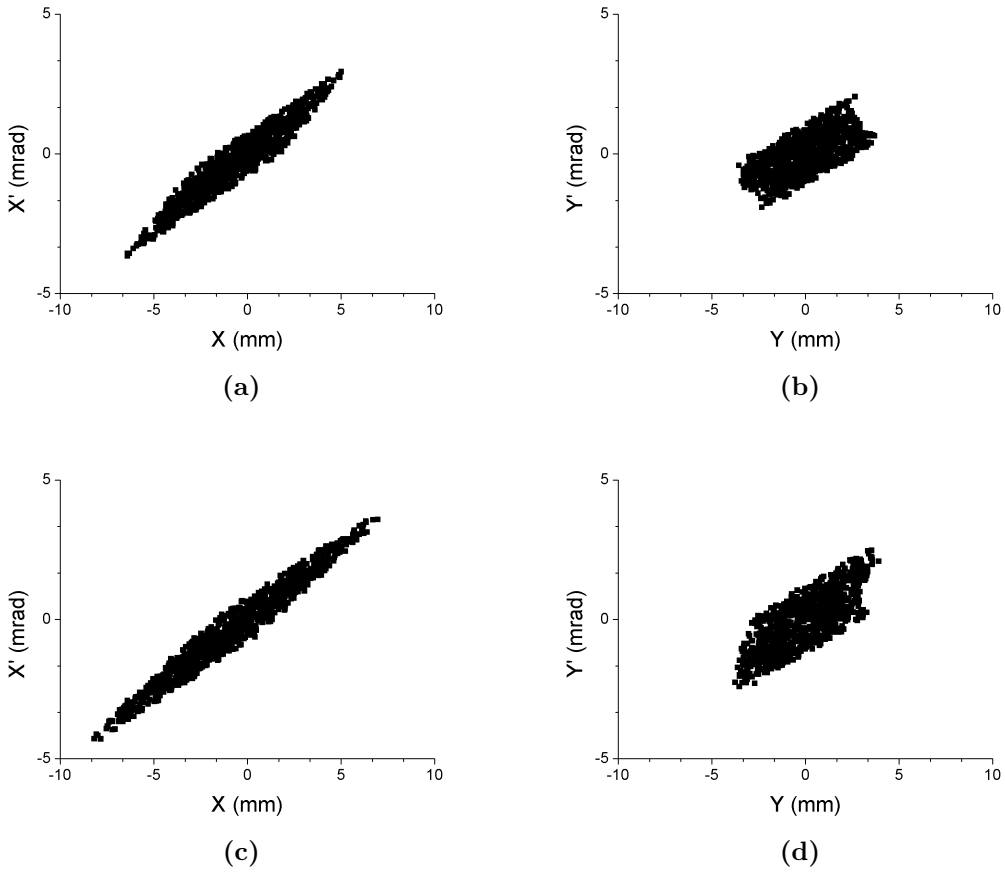

Figure 5.12: Emittance of the beam without any voltage applied on the CEC (a),(b), and with a high voltage applied (+10.000V) (c),(d).The volume remains unchanged but the beam becomes faster bigger with the high positive voltage applied because the beam is slowed down. Because of this there are some additional losses in the transmission when high positive voltages are applied.

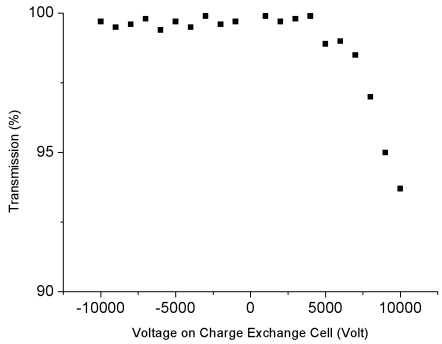

Figure 5.13: Transmission in function of applied voltages on the CEC - Transmission to the detection setup in function of applied voltages on the CEC. For all negative and small positive voltages the total transmission stays constant around 99%-100% but for higher positive voltages the total transmission drops off to 94%.

5.10 Bending towards detection

The last major part in the simulations is the deflection of the resonantly ionized ions toward the detection setup. This is done by two parallel bending electrodes. In the original design the plates where only 16mm apart from each other and were situated in the middle of the vacuum chamber. With this configuration it was impossible to bend the beam without losing a big part of the ions. Because the plates are so close to each other the ion beam hits the electrode if the bending angle is more than 10° (see figure 5.14). This problem was solved by putting

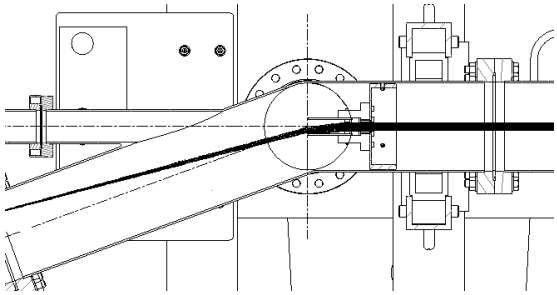

Figure 5.14: Beam hits bending electrodes - The plates are too close together and it is impossible to bend the beam enough to reach the detection setup

the plates further apart from each other: 32mm instead of 16mm. This way it was possible to bend the beam over an angle of 20°(see figure 5.15). . The

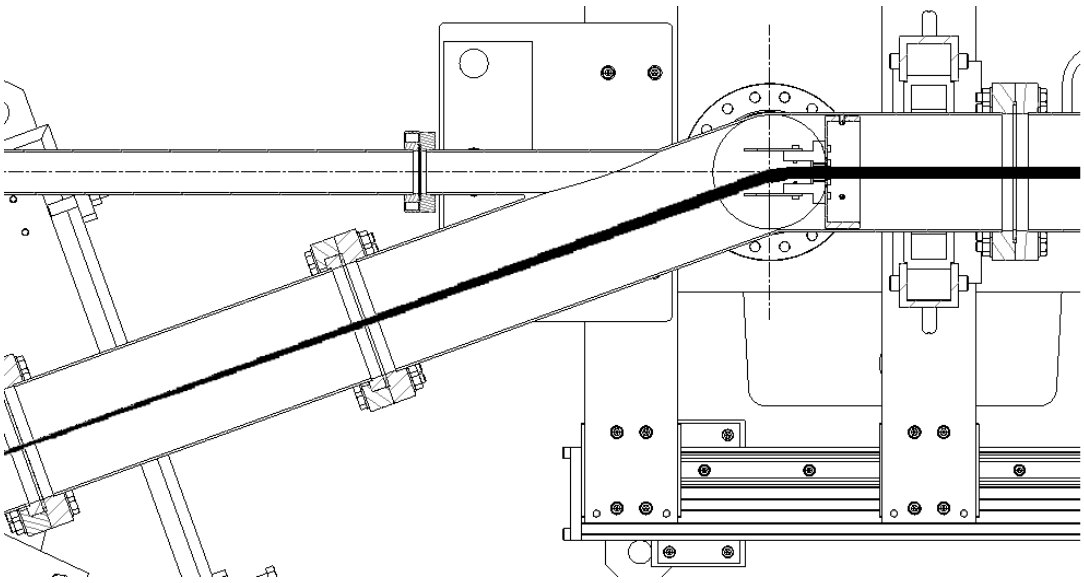

Figure 5.15: Plates 32mm apart - With the plates moved further away from each other, the beam can be bent over an angle of 20°

temporary detection setup consisting of an Micro Channel Plate detector (MCP) and a metal plate at which the ions impinge, whereby some electrons are released. These electrons are detected by the MCP. The metal plate is off centre in the beamline, therefore a bending angle slightly smaller than 20° is needed, so less high voltages have to be applied. There is a linear dependence between the voltage that has to be applied and the energy of the beam (see figure 5.16). While doing measurements the voltages on the bend have to be changed together with the scanning voltage that is applied on the charge exchange cell.

.

5.11 Total transmission

The transmission of the ion beam from the start of the experiment to the detection setup depends heavily on the ion optics elements used (see figure 5.17). With all optimal settings and no scanning voltage, the total transmission is around

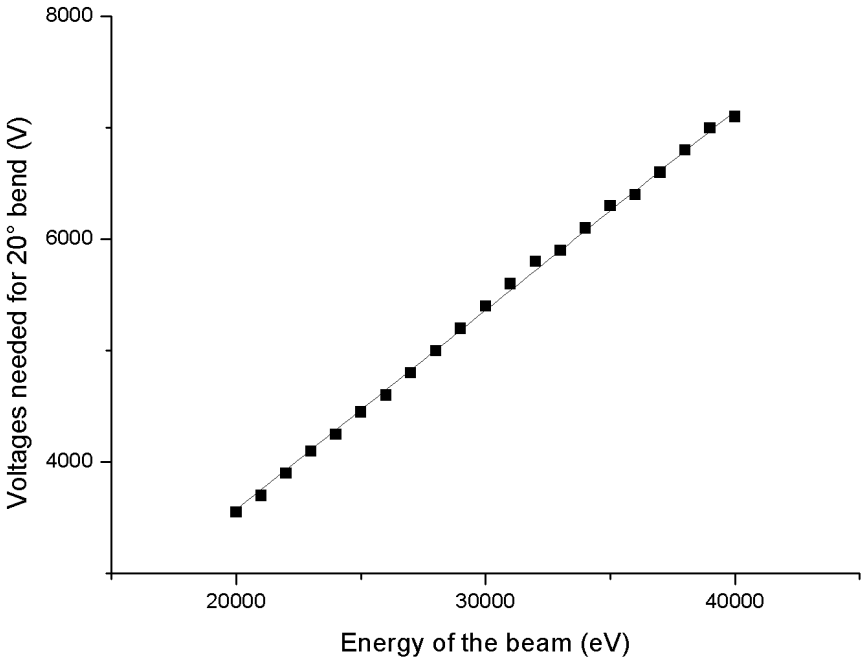

Figure 5.16: 20° bend - Plot of energy of the ion beam versus the voltage needed to bend over 20°

98.4% with only minor losses at the pumping apertures. Without the quadrupole doublet 40% of the beam is lost in the charge exchange cell, while another 40% is lost at the pumping apertures leaving only 20% total transmission. Without the extra bending plates after the 34° bend no particles reached the detection setup.

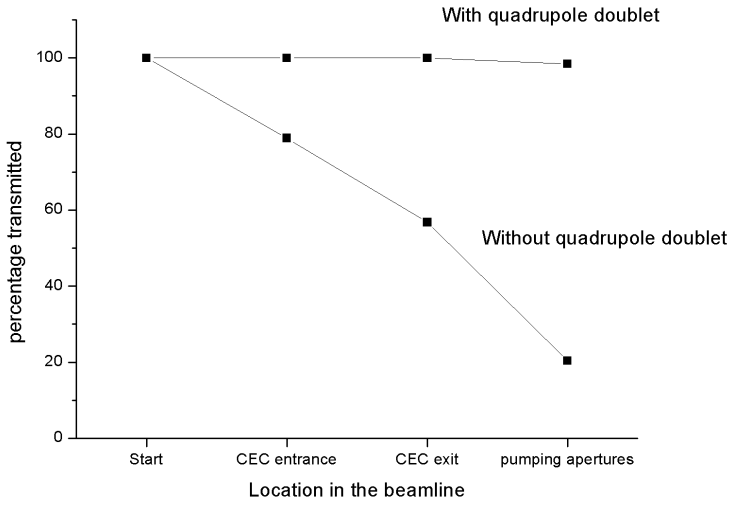

Figure 5.17: Total transmission - The total transmission through the beamline. The most important losses are in the Charge exchange cell and the pumping apertures.

6

Conclusions

The goal of this thesis was to simulate the ion optics and ion transmission of the new CRIS beamline at ISOLDE, CERN. The new beamline was already designed when this work started in April 2009, but construction had only just begun. No simulations for the ion optics had been done yet, and the beamline was thus not yet optimized for the transmission of the ions. In an experiment like CRIS that has a potentially very hight detection sensitivity, it is necessary to minimize the losses in the setup, because this will drastically reduce the sensitivity. Therefore simulations for the beam transport and ion optics were indispensable.
The effects of all the ion optic elements on the beam were investigated, and also the effect of the properties of the ion beam itself are taken into account.
Effects of the existing ion optic elements on the beam and the transmission is examined. First of all the quadrupole triplet that is used for focussing the ion beam coming from ISOLDE was simulated. The beam coming from ISOLDE is diverging, and has to be focused again to prevent it from becoming too big, which would result in partial loss of the ion beam. Then the ion beam has to be bent to make it overlap with the laser. Important here, is that it overlaps as much as possible to achieve a maximum interaction between the ion beam and the atoms. Here rose a first important problem: the ion beam was off centre which would result in complete beam loss. This problem was solved by adding extra bending plates in the beamline to correct. Another problem was the divergence of the ion beam, the bending plates act as a lens, and focus the ion beam. To compensate this, an additional quadrupole doublet was added to the setup. This doublet is

used to correct the focussing effect of the 34°, because after the charge exchange cell, where the ions are neutralised, there is a long drift region where the atoms can not be manipulated or the flight path corrected. The voltages that are put on the charge exchange cell can result in some additional beam loss, but only in cases where high positive voltages are applied this leads to noticeable losses. A last element in the simulations is the bending of the ion beam toward the detection setup. The design of the bending plates was not optimal, but this was easily resolved. All together this makes it possible to get a high transmission of the ion beam to the detection setup.

References

[Alk92] G. D. Alkhazov *et al.* A new highly efficient method of atomic spectroscopy for nuclides far from stability. *Nuclear Instruments and Methods in Physics Research B*, 69:517–520, 1992.

[Cam02] P. Campbell *et al.* Laser spectroscopy of cooled zirconium fission fragments. *Phys. Rev. Lett.*, 89(8), 2002.

[Jok03] A. Jokinen *et al.* Rfq-cooler for low-energy radioactive ions at isolde. *Nucl. Instr. and Meth. in Phys. Res. B*, 204:8689, 2003.

[Kau76] S.L. Kaufman. High-resolution laser spectroscopy in fast beams. *Optics Communications*, 17(3):309–312, 1976.

[Kin84] W. H. King. *Isotope Shift in Atomic Spectra*. New York (N.Y.): Plenum, 1984.

[Kud82] Yu. A. Kudriavtsev and V. S. Letokho. Laser method of highly selective detection of rare radioactive isotopes through multistep photoionization of accelerated atoms. *Appl. Phys.*, 29:219–221, 1982.

[Man09] E. Man *et al.* An ion cooler-buncher for high-sensitivity collinear laser spectroscopy at isolde. *Eur. Phys. J. A*, 42:503507, 2009.

[Neu06] R. Neugart and G. Neyens. Nuclear moments. *Lecture Notes in Physics*, 700:135–189, 2006.

[Ney03] G. Neyens. Nuclear magnetic and quadrupole moments for nuclear structure research on exotic nuclei. *Rep. Prog. Phys.*, 66:633–689, 2003.

[Ory09] G. Ory. Onderzoek naar de isotopenverschuiving van neutronrijke koperkernen met behulp van collineaire laser spectroscopie. Master's thesis, K.U. Leuven, 2009.

[Pod06] Ivan Podadera Aliseda. *New developments on preparation of cooled and bunched radioactive ion beams at ISOL-facilities: The ISCOOL project and the rotating wall cooling.* PhD thesis, CERN, Geneva, 2006.

[RIL] Rilis. http://isolde-project-rilis.web.cern.ch/isolde-project-rilis/intro/motivation.html.

[Sch91] Ch. Schulz *et al.* Resonance ionization spectroscopy on a fast atomic ytterbium beam. *J. Phys. B At. Mol. Opt. Phys*, 24:4831–4844, 1991.

[Sel69] E. C. Seltzer. K x-ray isotope shifts. *Phys. Rev.*, 188:1916, 1969.

[SIM] Simion. http://simion.com.

[Win76] W.H. Wing *et al.* Observation of the infrared spectrum of the hydrogen molecular ion hd+. *Phys. Rev. Lett.*, 36(25):14881491, 1976.

[Wol87] Hermann Wollnik. *Optics of Charged Particles.* Academic Press, Inc., 1987.